Acta Crystallographica Section F
Structural Biology and Crystallization Communications
ISSN 1744-3091

Crystallization and preliminary X-ray diffraction analysis of dihydrodipicolinate synthase 2 from *Arabidopsis thaliana*

Michael D. W. Griffin,[a]* Jagan M. Billakanti,[b] Juliet A. Gerrard,[b] Renwick C. J. Dobson[a,b] and F. Grant Pearce[b]

[a]Department of Biochemistry and Molecular Biology, Bio21 Molecular Science and Biotechnology Institute, The University of Melbourne, 30 Flemington Road, Parkville, Victoria 3010, Australia, and [b]Biomolecular Interaction Centre and School of Biological Sciences, University of Canterbury, Private Bag 4800, Christchurch, New Zealand

Correspondence e-mail: mgriffin@unimelb.edu.au

Received 22 June 2011
Accepted 16 August 2011

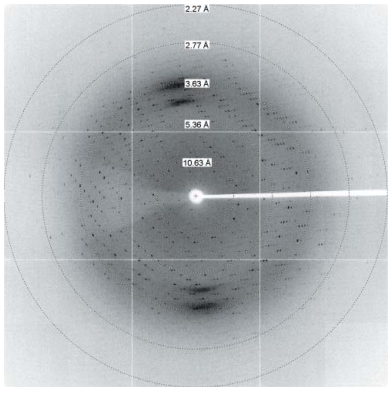

Dihydrodipicolinate synthase (DHDPS; EC 4.2.1.52) catalyzes the first committed step of the lysine-biosynthetic pathway in plants and bacteria. Since (*S*)-lysine biosynthesis does not occur in animals, DHDPS is an attractive target for rational antibiotic and herbicide design. Here, the cloning, expression, purification, crystallization and preliminary X-ray diffraction analysis of DHDPS2 from *Arabidopsis thaliana* are reported. Diffraction-quality protein crystals belonged to space group $P2_12_12$.

1. Introduction

The essential amino acid (*S*)-lysine is synthesized *via* two routes. One pathway uses the intermediate α-aminoadipic acid, which occurs in some fungi and in a few species from the kingdom Archaea (Nishida *et al.*, 1999; Velasco *et al.*, 2002). The other pathway utilizes the intermediate *meso*-diaminopimelate (*m*-DAP). This pathway is present in most bacterial species and photosynthetic organisms.

There are four variants of the *meso*-diaminopimelate/(*S*)-lysine pathway; they all share the same enzymatic steps for the synthesis of tetrahydrodipicolinate (THDPA) from aspartate (Hudson *et al.*, 2006), which includes the reaction catalyzed by dihydrodipicolinate synthase (DHDPS; EC 4.2.1.52). DHDPS catalyzes the branch-point reaction in the biosynthetic pathway leading to *meso*-diaminopimelate (*meso*-DAP) and (*S*)-lysine in plants and bacteria: condensation of (*S*)-aspartate-β-semialdehyde [(*S*)-ASA] and pyruvate to form (4*S*)-4-hydroxy-2,3,4,5-tetrahydro-(2*S*)-dipicolinic acid (HTPA) (Fig. 1; Dobson *et al.*, 2004).

Following reduction of HTPA to THDPA by dihydrodipicolinate reductase (DapB) (Fig. 1), most bacteria use acetylated or succinylated intermediates to convert THDPA to L,L-DAP, employing the enzymes tetrahydrodipicolinate acylase (DapD), acyl-amino-ketopimelate aminotransferase (DapC) and acyl-ketopimelate deacylase (DapE). Another variant of the pathway utilizes the enzyme diaminopimelate dehydrogenase (DapDh), which converts THDPA to *meso*-DAP in a single step, bypassing the acetyl/succinyl and L,L-DAP intermediates. The recently discovered diaminopimelate aminotransferase (DapL) pathway synthesizes L,L-DAP from THDPA (Hudson *et al.*, 2006; Dobson *et al.*, 2011). The conversion of diaminopimelate to (*S*)-lysine, catalyzed by the enzyme diaminopimelate decarboxylase (LysA), is the ultimate step in the pathway and this enzymatic reaction is common to all four variants.

Given that animals do not possess the machinery necessary for the *de novo* biosynthesis of lysine, enzymes associated with this pathway are attractive targets for the development of antibiotics, herbicides and algaecides. Accordingly, we have been engaged in the study of the structure and function of enzymes of lysine biosynthesis from a variety of pathogens (Atkinson *et al.*, 2009; Burgess, Dobson, Dogovski *et al.*, 2008; Burgess, Dobson, Bailey *et al.*, 2008; Dobson *et al.*, 2005, 2008; Kefala *et al.*, 2008; Voss *et al.*, 2009, 2010; Devenish *et al.*, 2008; Griffin *et al.*, 2008, 2010) and, in particular, the rational design of inhibitors against these enzymes (Boughton, Dobson *et al.*, 2008; Boughton, Griffin *et al.*, 2008; Mitsakos *et al.*, 2008; Turner *et al.*, 2005). In addition, many crop plants contain low levels of essential amino acids; cereals, in particular, have limiting amounts of lysine

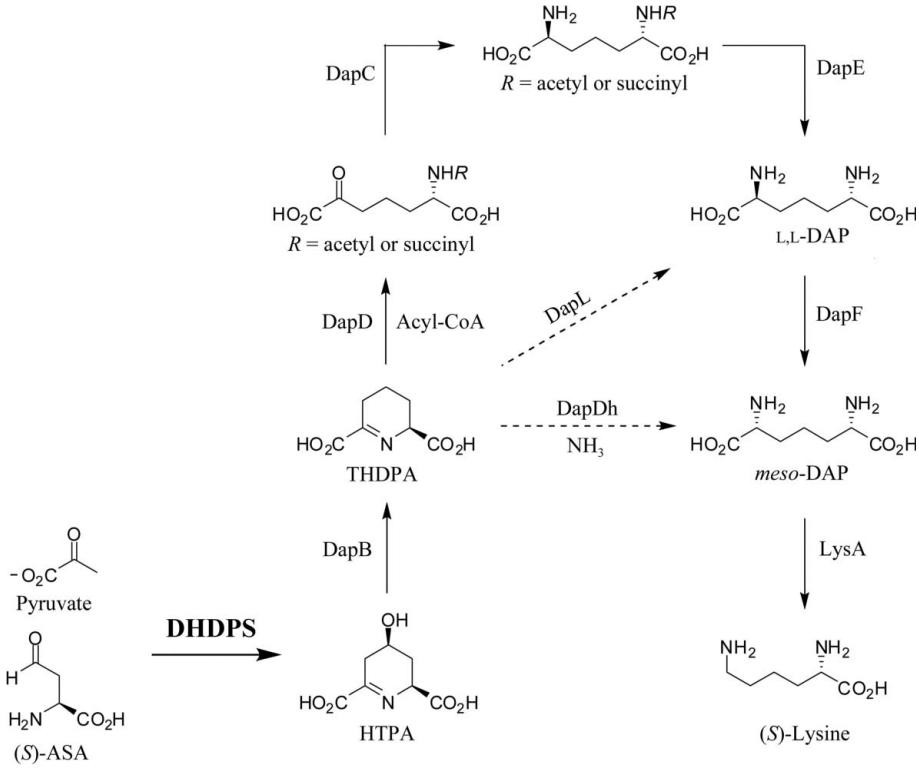

Figure 1
Lysine-biosynthetic pathways. The abbreviations for the enzymes are as follows: DapB, dihydrodipicolinate reductase; DapD, tetrahydrodipicolinate acylase; DapC, acyl-amino-ketopimelate aminotransferase; DapE, acyl-ketopimelate deacylase; DapF, diaminopimelate epimerase; LysA, diaminopimelate decarboxylase; DapDh, *meso*-diaminopimelate dehydrogenase; DapL, L,L-diaminopimelate aminotransferase. The abbreviations for the compounds are as follows: (*S*)-ASA, (*S*)-aspartate-β-semialdehyde; HTPA, (4*S*)-4-hydroxy-2,3,4,5-tetrahydro-(2*S*)-dipicolinic acid; THDPA, tetrahydrodipicolinate; DAP, diaminopimelate.

(Falco *et al.*, 1995; Silk & Matthews, 1997). Therefore, (*S*)-lysine biosynthesis is of interest to plant biotechnologists in the context of up-regulating (*S*)-lysine biosynthesis in plants (Shaul & Galili, 1992).

The crystal structures of DHDPS from a range of bacterial species have been solved (Kaur *et al.*, 2011; Kang *et al.*, 2010; Padmanabhan *et al.*, 2009; Devenish *et al.*, 2009; Rice *et al.*, 2008; Girish *et al.*, 2008; Phenix *et al.*, 2008; Dobson *et al.*, 2005; Burgess, Dobson, Bailey *et al.*, 2008; Blickling, Renner *et al.*, 1997). With the exception of the recently reported dimeric DHDPS enzymes from *Staphylococcus aureus* (Burgess, Dobson, Bailey *et al.*, 2008; Burgess, Dobson, Dogovski *et al.*, 2008; Girish *et al.*, 2008) and *Pseudomonas aeruginosa* (Kaur *et al.*, 2011), all functionally and structurally characterized bacterial DHDPS enzymes are homotetramers comprising a dimer-of-dimers structure.

Obtaining crystal structures of plant DHDPS enzymes has proved to be more challenging. The only reported crystal structure of DHDPS from a plant source is that of *Nicotiana sylvestris* at 2.80 Å resolution (Blickling, Beisel *et al.*, 1997); however, coordinate and structure-factor files were not deposited in the PDB. This structure displayed a striking rearrangement of the quaternary architecture of the enzyme in comparison to the bacterial enzymes, despite otherwise high structural homology. In addition, plant DHDPS enzymes are more sensitive to allosteric feedback inhibition by (*S*)-lysine than their bacterial counterparts and it has been proposed that the altered oligomeric configuration may account for this (Blickling, Beisel *et al.*, 1997), although this has yet to be confirmed.

To enhance our structural and functional understanding of plant DHDPS enzymes, we report here the cloning, expression, purification, crystallization and preliminary X-ray diffraction analysis (to 2.5 Å resolution) of DHDPS2 from *Arabidopsis thaliana* (*At*-DHDPS2).

2. Materials and methods

2.1. Cloning the *A. thaliana dap*A gene

A plasmid encoding AT2G45440 (DHDPS2) was obtained from the Arabidopsis Information Resource (TAIR), Carnegie Institution of Washington, Stanford, California, USA. Primer pairs encoding the predicted 5′–3′ ends of the desired ORF were used to amplify the gene. Primers were designed to exclude the chloroplast transit peptide as identified using *ChloroP* (Emanuelsson *et al.*, 1999) (forward, 5′-CACCGCAGCTGTTGTACCCAATTTCCATCTCCC-AATGC-3′; reverse, 5′-CTAATATCGACCGATAAAATCATCAT-CATCAAG-3′). The PCR product was ligated into the pET151/D-Topo vector (Invitrogen) and reactions were carried out using the manufacturer's protocols.

2.2. Expression and purification

Protein expression was performed in BL21 (DE3) Star cells using ZYM-5052 medium (Studier, 2005). Cultures were grown at 310 K for 5 h followed by incubation at 299 K overnight. Cells were harvested by centrifugation, resuspended in buffer consisting of 50 m*M* NaH_2PO_4 pH 8.0, 30 m*M* imidazole and 300 m*M* NaCl and lysed by sonication. Cell debris was pelleted by centrifugation and the cell pellet was applied to a His-Trap Crude column (GE Biosciences). The column was washed with three volumes of resuspension buffer before bound protein was eluted using 50 m*M* NaH_2PO_4 pH 8.0, 300 m*M*

imidazole and 300 m*M* NaCl. Fractions containing protein were desalted into 20 m*M* Tris–HCl pH 8.0 for storage.

2.3. Mass spectrometry

Mass spectrometry was performed using an Agilent time-of-flight mass spectrometer equipped with an ESI source (ESI-TOF). Protein samples (5 µl) were directly infused at a flow rate of 250 µl min^{-1} *via* a line containing 0.1% formic acid in 50% acetonitrile. Mass-spectral data were deconvoluted and analyzed using the program *Mass Hunter* (Agilent).

2.4. Crystallization

Crystallization screens were conducted as described previously (Voss *et al.*, 2009; Dobson *et al.*, 2008; Burgess, Dobson, Dogovski *et al.*, 2008). Protein crystallization experiments were performed at the Bio21 Collaborative Crystallization Centre (C^3; CSIRO, Parkville, Melbourne) using the PACT Suite and the JCSG+ suite of crystal screens at 281 and 293 K (Newman *et al.*, 2005, 2008). The screens were set up using the sitting-drop vapour-diffusion method. Crystals used for data collection were obtained at 293 K from a 300 nl drop formed from 150 nl *At*-DHDPS2 solution (14.5 mg ml^{-1} in 20 m*M* Tris–HCl pH 8.0) and 150 nl reservoir solution [PACT condition D7; 20%(*w*/*v*) PEG 6000, 200 m*M* sodium chloride, 100 m*M* Tris–HCl pH 8.0 including 0.02%(*w*/*v*) sodium azide].

2.5. Data collection and processing

For X-ray data collection, *At*-DHDPS2 crystals were briefly soaked in cryoprotectant solution consisting of reservoir solution made up to 10%(*v*/*v*) glycerol and 10%(*v*/*v*) ethylene glycol and flash-cooled in liquid nitrogen. Intensity data were collected at 110 K using the MX2 beamline at the Australian Synchrotron. Images were collected in 1.0° rotations over 120° using an ADSC Q315r CCD (crystal-to-detector distance of 350 mm) with an exposure time of 2.0 s and 80% beam attenuation. The diffraction images were processed using the programs *MOSFLM* (Leslie, 1992) and *XDS* (Kabsch, 2010). The resulting intensity data sets were analyzed using *POINTLESS* (Evans, 2006) and scaled and merged using *SCALA* (Evans, 2006). Images will be made available *via* the TARDIS server (Androulakis *et al.*, 2008) when the structure is published. Molecular replacement was performed using the program *Phaser* (Adams *et al.*, 2010) as implemented in *PHENIX* (Adams *et al.*, 2010).

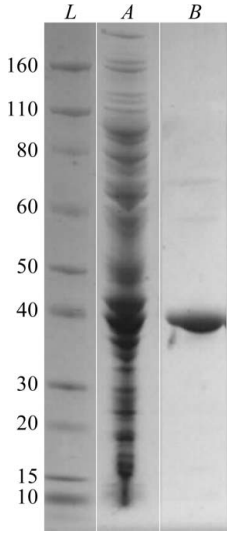

Figure 2
SDS–PAGE of purified *At*-DHDPS2. Lane *L*, mass markers (kDa); lane *A*, crude lysate; lane *B*, purified *At*-DHDPS.

3. Results and discussion

3.1. Cloning, expression and purification of *At*-DHDPS2

The gene encoding *At*-DHDPS2 was successfully cloned from the AT2G45440 ORF. The final construct lacked a 38-amino-acid chloroplast transit peptide present in the original ORF and contained a C-terminal His tag with a TEV cleavage site. Purification was carried out using nickel-affinity chromatography, yielding a pure protein sample (>95% as judged by SDS–PAGE; Fig. 2).

Mass-spectrometric analysis of the sample prior to crystallization screening revealed that the major species in solution (approximately 65% of the total protein) had a mass of 34 679.89 Da (Fig. 3) corresponding to the predicted mass for residue 46 to the C-terminus of the full-length construct. This indicates specific cleavage of the freshly purified full-length protein after Arg45, which is a predicted protease II cleavage site (Kanatani *et al.*, 1991). Thus, it appears that trace proteases may have been present in the purified protein preparation and that the N-terminus of the protein is particularly susceptible to proteolysis. Since proteolysis should continue during the incubation of crystallization experiments, the proportion of this specific cleavage product within the crystallization drops would increase further over time.

3.2. Crystallization of *At*-DHDPS2 and X-ray diffraction data collection

Purified *At*-DHDPS2 protein was screened for crystallization using the JCSG+ and PACT screens at 281 and 293 K. Crystals appeared rapidly in many conditions containing 20% PEG 3350 with various inorganic salts at above neutral pH. However, the diffraction data obtained from these crystals were weak and were limited to around 5 Å resolution, indicating that these crystals were unsuitable for structure solution.

Crystals appeared after 5 d in drops consisting of 20%(*w*/*v*) PEG 6000, 200 m*M* sodium chloride, 100 m*M* HEPES pH 7.0. On close

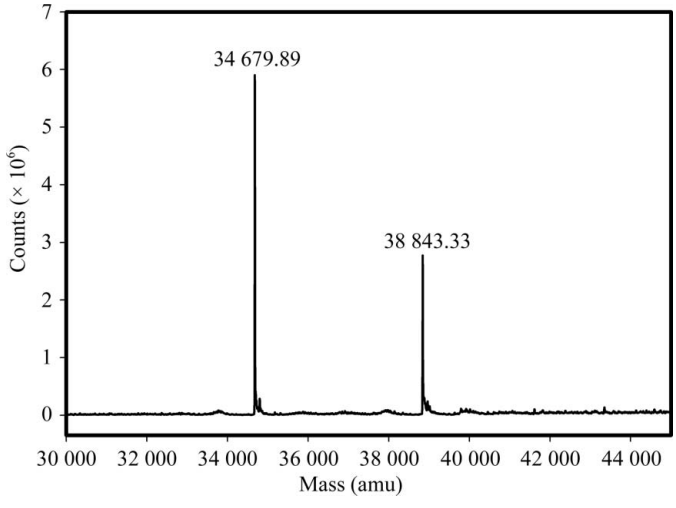

Figure 3
Deconvoluted mass spectrum of *At*-DHDPS2 used for crystallization experiments. Proteolysis of the full-length protein to form the major mass species of 34 679.89 Da occurred during storage of the protein at 277 K.

inspection, these crystals appeared to be composed of many long separate domains oriented obliquely to the long axis of the crystal. Diffraction data collected from these crystals showed weak diffraction to beyond 3 Å resolution with many overlapping diffraction patterns, confirming the presence of multiple domains. Grid optimization of these conditions failed to produce crystals of improved quality.

After approximately eight weeks, plate-shaped crystals (up to ∼10 × 60 × 120 µm) grew in drops containing 20%(*w*/*v*) PEG 6000, 200 m*M* sodium chloride, 100 m*M* Tris–HCl pH 8.0. The crystals were clear, rhomboid in shape in their larger dimensions and of constant thickness. Facets were well formed and the crystals were separated with no outward signs of penetrative twinning. These crystals showed good diffraction to beyond 2.5 Å resolution with visible spot smearing on higher resolution reflections (Fig. 4). For all crystals, the resolution and the quality of diffraction was highly dependent on the section of the crystal illuminated by the X-ray beam, with the edges generally showing the best diffraction. Diffraction experiments were conducted using the microfocus MX2 beamline of the Australian Synchrotron to facilitate the collection of the best possible data. Nevertheless, significant fluctuations in diffraction quality were unavoidable during crystal rotation and evidence of radiation damage was observed in later images. The rotation range of the data used for processing was therefore chosen to maximize data quality while retaining high data completeness.

3.3. X-ray diffraction data processing and molecular-replacement solution

Diffraction images were indexed and integrated in space group *P*222 using *MOSFLM* and *XDS*. Analysis of the intensity data using *POINTLESS* indicated that the crystals belonged to space group $P2_122_1$, with unit-cell parameters *a* = 56.2, *b* = 69.4, *c* = 147.5 Å. Matthews coefficients calculated for the protein masses obtained from mass spectrometry (34 679.89 and 38 843.33 Da; Fig. 3) suggest

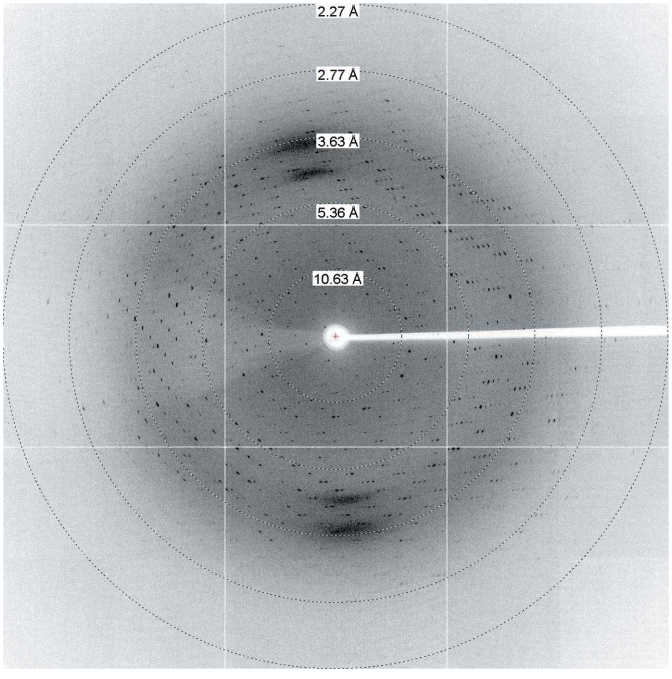

Figure 4
X-ray diffraction image of *At*-DHDPS2 displaying the quality of the reflections out to 2.5 Å resolution.

Table 1
X-ray data-collection statistics for *At*-DHDPS2.

Values in parentheses are for the highest resolution shell. The Matthews coefficient and the estimate of the solvent content are based on a molecular weight of 69 359 Da in the asymmetric unit (two molecules of *At*-DHDPS2 of 34 679.5 Da each).

Wavelength (Å)	0.96369
No. of images	120
Oscillation (°)	1.0
Space group	$P2_12_12$
Unit-cell parameters (Å)	*a* = 147.5, *b* = 56.2, *c* = 69.4
Resolution (Å)	19.73–2.50 (2.64–2.50)
Observed reflections	98313
Unique reflections	20590
Completeness (%)	99.7 (99.9)
$R_{\rm merge}$†	0.122 (0.637)
$R_{\rm p.i.m.}$‡	0.061 (0.316)
$R_{\rm r.i.m.}$§	0.137 (0.713)
Mean $I/\sigma(I)$	12.2 (2.7)
Multiplicity	4.8 (4.9)
Wilson *B* value (Å^2)	41.0
Estimated molecules in asymmetric unit	2
$V_{\rm M}$ (Å^3 Da^{-1})	2.07
Solvent content (%)	40.7

† $R_{\rm merge} = \sum_{hkl}\sum_i |I_i(hkl) - \langle I(hkl)\rangle| / \sum_{hkl}\sum_i I_i(hkl)\sum_{hkl}$. ‡ $R_{\rm pim} = \sum_{hkl}[1/(N-1)]^{1/2} \times \sum_i |I_i(hkl) - \langle I(hkl)\rangle| / \sum_{hkl}\sum_i I_i(hkl)$. § $R_{\rm rim} = \sum_{hkl}[N/(N-1)]^{1/2}\sum_i |I_i(hkl) - \langle I(hkl)\rangle| / \sum_{hkl}\sum_i I_i(hkl)$.

that the smaller, proteolyzed protein is more compatible with this unit cell (Table 1), since the larger species corresponds to a Matthews coefficient of 1.85 Å^3 Da^{-1}. Systemic absences in the axial reflections were consistent with the presence of only two screw axes.

Scaling and merging the intensity data sets using *SCALA* resulted in significantly better merging statistics from the data integrated using *XDS* in comparison to those obtained using *MOSFLM*. This is presumably owing to the improved ability of *XDS* to handle spot smearing by three-dimensional profile fitting. The data-collection and processing statistics for the *XDS* data set are summarized in Table 1.

Molecular replacement was performed using the program *Phaser* with the monomer of DHDPS from *N. sylvestris* as the search model (Blickling, Beisel *et al.*, 1997) and assuming the presence of two monomers in the asymmetric unit. Initially, data scaled in space group *P*222 were used and all compatible space groups were searched. A single correct solution was found in $P2_122_1$, providing further evidence that this was the correct space group. Thus, the data were re-indexed and scaled in reference space group $P2_12_12$, with unit-cell parameters *a* = 147.5, *b* = 56.2, *c* = 69.4 Å. The search model was improved using the program *CHAINSAW* (Stein, 2008), retaining all side-chain atoms common to *N. sylvestris* DHDPS and *At*-DHDPS2. Molecular replacement with this search model using the data indexed in $P2_12_12$ produced a final solution with a translation-function *Z* score (TFZ) of 38.9. Refinement of the structure of *At*-DHDPS2 is currently under way.

MDWG is the recipient of an Australian Research Council Post-Doctoral Fellowship (project No. DP110103528). RCJD acknowledges the C. R. Roper Bequest for fellowship support and the New Zealand Royal Society Marsden Fund for funding support (UOC1013). JMB and FGP were supported by the Defence Threat Reduction Agency (W911NF-07-1-0073 and AB07CBT004) and in part by the Foundation of Research, Science and Technology. Travel to the Australian Synchrotron was supported by the New Zealand Synchrotron Group. We would also like to acknowledge the support and assistance of the friendly staff, especially Dr Janet Newman, at the Bio21 Collaborative Crystallographic Centre at CSIRO Molecular and Health Technologies, Parkville, Melbourne, Australia. Part

of this research was undertaken on the MX2 beamline at the Australian Synchrotron, Victoria, Australia.

References

Adams, P. D. *et al.* (2010). *Acta Cryst.* D**66**, 213–221.
Androulakis, S. *et al.* (2008). *Acta Cryst.* D**64**, 810–814.
Atkinson, S. C., Dobson, R. C. J., Newman, J. M., Gorman, M. A., Dogovski, C., Parker, M. W. & Perugini, M. A. (2009). *Acta Cryst.* F**65**, 253–255.
Blickling, S., Beisel, H. G., Bozic, D., Knäblein, J., Laber, B. & Huber, R. (1997). *J. Mol. Biol.* **274**, 608–621.
Blickling, S., Renner, C., Laber, B., Pohlenz, H. D., Holak, T. A. & Huber, R. (1997). *Biochemistry*, **36**, 24–33.
Boughton, B. A., Dobson, R. C. J., Gerrard, J. A. & Hutton, C. A. (2008). *Bioorg. Med. Chem. Lett.* **18**, 460–463.
Boughton, B. A., Griffin, M. D. W., O'Donnell, P. A., Dobson, R. C. J., Perugini, M. A., Gerrard, J. A. & Hutton, C. A. (2008). *Bioorg. Med. Chem.* **16**, 9975–9983.
Burgess, B. R., Dobson, R. C. J., Bailey, M. F., Atkinson, S. C., Griffin, M. D. W., Jameson, G. B., Parker, M. W., Gerrard, J. A. & Perugini, M. A. (2008). *J. Biol. Chem.* **283**, 27598–27603.
Burgess, B. R., Dobson, R. C. J., Dogovski, C., Jameson, G. B., Parker, M. W. & Perugini, M. A. (2008). *Acta Cryst.* F**64**, 659–661.
Devenish, S. R. A., Gerrard, J. A., Jameson, G. B. & Dobson, R. C. J. (2008). *Acta Cryst.* F**64**, 1092–1095.
Devenish, S. R. A., Huisman, F. H., Parker, E. J., Hadfield, A. T. & Gerrard, J. A. (2009). *Biochim. Biophys. Acta*, **1794**, 1168–1174.
Dobson, R. C. J., Atkinson, S. C., Gorman, M. A., Newman, J. M., Parker, M. W. & Perugini, M. A. (2008). *Acta Cryst.* F**64**, 206–208.
Dobson, R. C. J., Girón, I. & Hudson, A. (2011). *PLoS One*, **6**, e20439.
Dobson, R. C. J., Griffin, M. D. W., Jameson, G. B. & Gerrard, J. A. (2005). *Acta Cryst.* D**61**, 1116–1124.
Dobson, R. C. J., Valegård, K. & Gerrard, J. A. (2004). *J. Mol. Biol.* **338**, 329–339.
Emanuelsson, O., Nielsen, H. & von Heijne, G. (1999). *Protein Sci.* **8**, 978–984.
Evans, P. (2006). *Acta Cryst.* D**62**, 72–82.
Falco, S. C., Guida, T., Locke, M., Mauvais, J., Sanders, C., Ward, R. T. & Webber, P. (1995). *Biotechnology*, **13**, 577–582.
Girish, T. S., Sharma, E. & Gopal, B. (2008). *FEBS Lett.* **582**, 2923–2930.
Griffin, M. D. W., Dobson, R. C. J., Gerrard, J. A. & Perugini, M. A. (2010). *Arch. Biochem. Biophys.* **494**, 58–63.
Griffin, M. D. W., Dobson, R. C. J., Pearce, F. G., Antonio, L., Whitten, A. E., Liew, C. K., Mackay, J. P., Trewhella, J., Jameson, G. B., Perugini, M. A. & Gerrard, J. A. (2008). *J. Mol. Biol.* **380**, 691–703.
Hudson, A. O., Singh, B. K., Leustek, T. & Gilvarg, C. (2006). *Plant Physiol.* **140**, 292–301.
Kabsch, W. (2010). *Acta Cryst.* D**66**, 125–132.
Kanatani, A., Masuda, T., Shimoda, T., Misoka, F., Lin, X. S., Yoshimoto, T. & Tsuru, D. (1991). *J. Biochem.* **110**, 315–320.
Kang, B. S., Kim, Y.-G., Ahn, J.-W. & Kim, K.-J. (2010). *Int. J. Biol. Macromol.* **46**, 512–516.
Kaur, N., Gautam, A., Kumar, S., Singh, A., Singh, N., Sharma, S., Sharma, R., Tewari, R. & Singh, T. P. (2011). *Int. J. Biol. Macromol.* **48**, 779–787.
Kefala, G., Evans, G. L., Griffin, M. D. W., Devenish, S. R. A., Pearce, F. G., Perugini, M. A., Gerrard, J. A., Weiss, M. S. & Dobson, R. C. J. (2008). *Biochem. J.* **411**, 351–360.
Leslie, A. G. W. (1992). *Jnt CCP4/ESF–EACBM Newsl. Protein Crystallogr.* **26**.
Mitsakos, V., Dobson, R. C. J., Pearce, F. G., Devenish, S. R., Evans, G. L., Burgess, B. R., Perugini, M. A., Gerrard, J. A. & Hutton, C. A. (2008). *Bioorg. Med. Chem. Lett.* **18**, 842–844.
Newman, J., Egan, D., Walter, T. S., Meged, R., Berry, I., Ben Jelloul, M., Sussman, J. L., Stuart, D. I. & Perrakis, A. (2005). *Acta Cryst.* D**61**, 1426–1431.
Newman, J., Pham, T. M. & Peat, T. S. (2008). *Acta Cryst.* F**64**, 991–996.
Nishida, H., Nishiyama, M., Kobashi, N., Kosuge, T., Hoshino, T. & Yamane, H. (1999). *Genome Res.* **9**, 1175–1183.
Padmanabhan, B., Strange, R. W., Antonyuk, S. V., Ellis, M. J., Hasnain, S. S., Iino, H., Agari, Y., Bessho, Y. & Yokoyama, S. (2009). *Acta Cryst.* F**65**, 1222–1226.
Phenix, C. P., Nienaber, K., Tam, P. H., Delbaere, L. T. & Palmer, D. R. J. (2008). *Chembiochem*, **9**, 1591–1602.
Rice, E. A., Bannon, G. A., Glenn, K. C., Jeong, S. S., Sturman, E. J. & Rydel, T. J. (2008). *Arch. Biochem. Biophys.* **480**, 111–121.
Shaul, O. & Galili, G. (1992). *Plant Physiol.* **100**, 1157–1163.
Silk, G. W. & Matthews, B. F. (1997). *Plant Mol. Biol.* **33**, 931–933.
Stein, N. (2008). *J. Appl. Cryst.* **41**, 641–643.
Studier, F. W. (2005). *Protein Expr. Purif.* **41**, 207–234.
Turner, J. J., Healy, J. P., Dobson, R. C., Gerrard, J. A. & Hutton, C. A. (2005). *Bioorg. Med. Chem. Lett.* **15**, 995–998.
Velasco, A. M., Leguina, J. I. & Lazcano, A. (2002). *J. Mol. Evol.* **55**, 445–459.
Voss, J. E., Scally, S. W., Taylor, N. L., Atkinson, S. C., Griffin, M. D. W., Hutton, C. A., Parker, M. W., Alderton, M. R., Gerrard, J. A., Dobson, R. C. J., Dogovski, C. & Perugini, M. A. (2010). *J. Biol. Chem.* **285**, 5188–5195.
Voss, J. E., Scally, S. W., Taylor, N. L., Dogovski, C., Alderton, M. R., Hutton, C. A., Gerrard, J. A., Parker, M. W., Dobson, R. C. J. & Perugini, M. A. (2009). *Acta Cryst.* F**65**, 188–191.